ACS OMEGA

http://pubs.acs.org/journal/acsodf

Article

A Novel Hydrate Form of Sodium Dodecyl Sulfate and Its Crystallization Process

Hung Lin Lee, Yun Sheng Cheng, Kuan Lin Yeh, and Tu Lee*

Cite This: *ACS Omega* 2021, 6, 15770−15781

Read Online

ACCESS | Metrics & More | Article Recommendations | Supporting Information

ABSTRACT: A novel hydrate form of sodium dodecyl sulfate (SDS) was firstly discovered through a hydrate screening with the use of organic solvents, while SDS is generally prepared solely in aqueous media. Surprisingly, a novel SDS hydrate form with needle-shaped crystals produced by adding acetonitrile to a 20 wt % SDS aqueous solution at a ratio of 3:1 (v/v) and further cooling to around 5 °C could be found with a trace amount in one of the two purchased SDS products that we examined. After comprehensive solid-state characterizations by powder X-ray diffraction (PXRD), thermogravimetric analysis (TGA), Fourier transform infrared (FTIR), Raman spectroscopy, dynamic vapor sorption (DVS), and elemental analysis (EA), it is also successfully made directly from the synthesis of SDS through esterification and saponification. Four times the equal proportion of acetone was added into the reaction solution at an interval of 5 min to separate the side product, sodium sulfate, from the mother liquor. The desired novel hydrate form of SDS was then obtained by cooling the filtered mother liquor to 5 °C and aged for 8 h for a preferential growth.

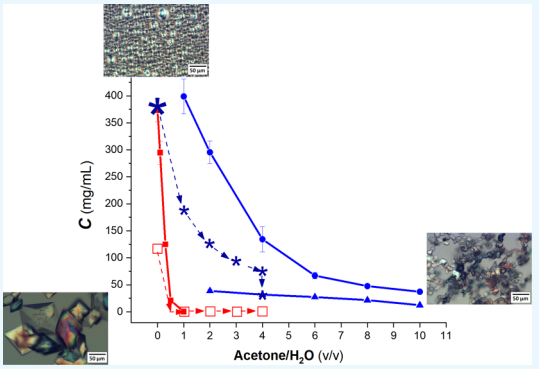

INTRODUCTION

Surfactants, or surface active agents, which are amphiphilic molecules, can considerably reduce the interfacial tension between two liquids or between a liquid and a gas or a solid. In general, surfactants fall into four classes, i.e., anionic, cationic, amphoteric, and nonionic, based on the charge of their hydrophilic headgroup. Anionic surfactants are mostly used in laundry detergents because most of the dirt, clay, and some oily stains are positively charged particles and are inclined to bind to anionic surfactants.

Sodium dodecyl sulfate (SDS) also called sodium lauryl sulfate (SLS), consisting of an alkyl tail of 12 carbon atoms attached to a sulfate group, is one of the very common anionic surfactants for the negative charge of its sulfate group. SDS is often used as a component in a variety of products, such as domestic cleaning, personal hygiene and cosmetic, pharmaceutical and food, or product formulations. It has also demonstrated wide applications in the separation of proteins for electrophoresis,[1] solubilization of proteins and lipids[2] as well as drugs,[3,4] dispersion of functionalized carbon nanotubes[5] and graphene sheets,[6] and formation of gas hydrate[7,8] and as an organic template for the formation of periodic mesoporous organosilica nanospheres.[9]

Solution crystallization often serves as a process or unit operation for manufacturing a wide range of crystalline substances, also including surfactants. However, for most crystallization processes, surfactants are used as an additive to modify crystal properties,[10−12] to assemble mesocrystals (three-dimensionally well-aligned nanosized particles),[13] or to affect nucleation and crystal growth through the manipulation of interfacial tension.[14] Only a few studies on surfactant crystallization itself were reported, and yet, a diversity of crystal attributes, such as polymorphs and pseudo-polymorphs, morphologies, and size distributions of a crystalline substance, have implications in downstream processing characteristics and product performance.[15−17] For instance, flowability, compressibility (i.e., tabletability), and dissolution rate are often considered for powdered detergents or tablets.[18] The understanding of surfactant crystallization can definitely help in the control of those attributes of a product surfactant for surfactant-based products, especially when the crystallization mechanisms for surfactant systems are complex. When the surfactant concentration is above the critical micelle concentration (CMC), its kinetic processes of micelle formation and crystal nucleation are competing with each other. Which of the two processes will be rate-limiting largely depends, to some extent, on the system examined and processing conditions.[19]

Polymorphism is a widespread phenomenon for more than half of all the drug substances in the pharmaceutical industry.[20]

Received: March 3, 2021
Accepted: May 31, 2021
Published: June 8, 2021

Surfactant formulations are often subjected to temperature variations or environmental changes, which may induce a polymorphic transformation, during manufacture, storage, transportation, and use and are expected to be stable across an extensive range of conditions. In addition to minimizing impurities in formulations, the instability due to the presence of different polymorphs (i.e., structural impurities) that is undesirable at all times for manufacturing and practical applications must be prevented. Since polymorphs as well as pseudo-polymorphs (i.e., solvates and hydrates) exhibit distinct physicochemical properties, it is necessary to explore surfactant crystallization in more detail for a better control over a purely specific (pseudo-)polymorph with consistent physicochemical properties. Moreover, knowledge of the water content of hydration is also essential for determining the equivalent weight and dosage amount in formulations.

SDS can occur in various hydrate forms depending on the concentration and temperature.[21−24] Those forms can interconvert from one another according to their thermodynamic stability in a given region or composition. Accordingly, stability, molecular weight, dissolution rate, hardness, toughness, and morphology of SDS solids would be greatly affected as its hydrate structure varies. Noticeably, it was said that the commercially purchased SDS solids are indeed a mixture of various hydrate forms rather than a specific hydrate form.[25] Moreover, SDS may undergo an autocatalytic, acid-catalyzed hydrolysis that produces 1-dodecanol and hydrogen sulfate, and its rate of hydrolysis is dependent on concentration, temperature, and pH.[26,27] Therefore, in the present study, we were the first to re-examine our purchased SDS products by several solid-state characterization tools, including powder X-ray diffraction (PXRD), thermogravimetric analysis (TGA), Fourier transform infrared (FTIR), Raman spectroscopy, dynamic vapor sorption (DVS), and elemental analysis (EA).

As the phase diagram of the SDS−water binary system had been well-established using differential scanning calorimetry (DSC), optical microscopy, nuclear magnetic resonance (NMR), and XRD,[28−30] the crystallization of SDS from aqueous solutions has also been investigated for several decades.[19,31−37] A weak dependence of cooling rate from 20 to 8 °C on the metastable zone width (MZW) was observed using optical microscopy and turbidimetry for the SDS crystallization in aqueous solutions of 5−20% SDS.[19,33] It implied that such SDS crystallization is dependent on solute exchange between the micelles and the monomers of SDS (i.e., the nucleating phase) particularly at a lower concentration. An unequivocal relationship between crystallization kinetics, morphologies, and polymorphs of SDS was interpreted using optical microscopy, DSC, and attenuated total reflection (ATR)-FTIR spectroscopy under isothermal conditions over a wide range of temperatures from 20 to −6 °C and concentrations of 10 to 30% SDS.[35] The results showed two kinds of pseudo-polymorphs as well as morphologies, including the needle-shaped SDS·hemihydrate, and platelet-shaped SDS·monohydrate, which dominates at ≤−2 °C, and relatively higher temperatures, respectively. Furthermore, nucleation and overall crystallization kinetics in 20% SDS aqueous solutions were described under linear cooling conditions over a range of temperatures from 22 to −5 °C with cooling rates ranging from 0.1 to 50 °C/min using optical microscopy and DSC based on Nývlt, and Avrami and Kissinger equations, respectively.[36]

However, such understanding of those SDS crystallization subjects was constrained to the "cooling" method, in aqueous solutions, and on a small scale, such as sealed capillary tubes,[19,35,36] or sample cells for various instruments, FTIR,[32] DSC,[35,36] dynamic light scattering (DLS) and small angle neutron scattering (SANS).[37] More recently, we have developed a controllable SDS crystallization process, which integrates evaporation, antisolvent addition, and cooling methods, to produce stable SDS·1/8 hydrate-specific solids.[25] The aims of the present study were to screen pseudo-polymorphs with the use of organic solvents, and to further develop the crystallization process directly following from the synthesis of SDS.

RESULTS AND DISCUSSION

Preparation of a Novel SDS Hydrate by Recrystallization. It has been discovered that SDS can exist in four hydrate forms for decades, i.e., 1/8 hydrate,[21] hemihydrate,[22] monohydrate,[23] and dihydrate. Except for SDS dihydrate, the crystal structures of the other SDS hydrates have been resolved by single crystal X-ray diffraction (SXD). Those hydrate forms, excluding SDS·1/8 hydrate, were prepared and formed in purely aqueous media. It was reported that its 1/8 hydrate is stable under normal conditions.[25,32] In addition, one crystal structure of the anhydrous SDS form has already been determined using a combination of synchrotron radiation powder diffraction and molecular modeling,[24] while SDS is apt to absorb and bind to water molecules in air at ambient conditions.

Because of SDS's importance of being a commercial product of surfactant, two kinds of purchased SDS solids were analyzed first by PXRD in the present study. One of the two was even labeled as "anhydrous SDS". Obviously, both are, in fact, a mixture of different SDS hydrates as shown in Figure 1. That can be regarded as structural impurities. As compared with the theoretical patterns of all known SDS structures (Figure 1c−f), the PXRD pattern of the purchased SDS (Figure 1a) shows a small, unknown peak at $2\theta \approx 7.5°$, also indicating a mixture of SDS hydrates. As a result, (pseudo-)polymorph screening of SDS was conducted for the unidentified diffraction peak. Also, the PXRD pattern of the purchased "anhydrous" SDS (Figure 1b) was treated as a mixture of hemihydrate, 1/8 hydrate, and anhydrous forms. Although some of the diffraction peaks for SDS·1/8 hydrate overlap with the ones for the anhydrous SDS form (Figure 1c,d) the characteristic peaks for SDS·1/8 hydrate can still be clearly observed. The TGA scans in Figure S1 confirm that the purchased "anhydrous" SDS solids are actually hydrates, rather than a specific hydrate, and could not be returned to a truly anhydrous form even after dehydration.

This may be due to the fact that SDS solids are traditionally made by spray drying.[38] A slurry or droplets of aqueous SDS solution are sprayed with a hot drying gas to rapidly evaporate off the liquid to produce fine SDS powder. Oftentimes, a short evaporation time like this makes it difficult to have a good control over the crystalline form of its product to be specific. SDS is highly soluble in water and forms micelles in aqueous solution above 8.2 mM, which is its CMC at 25 °C.[37,39] As the solute concentration of SDS in aqueous solution increases by reducing its water content, the SDS solution will pass through several complex phases of micelles, liquid crystals, and coagels toward the formation of a very thick slurry, causing poor mixing, and heat and mass transfer.[25] The strong affinity to water of those structures often makes the removal of water

https://doi.org/10.1021/acsomega.1c01147
ACS Omega 2021, 6, 15770−15781

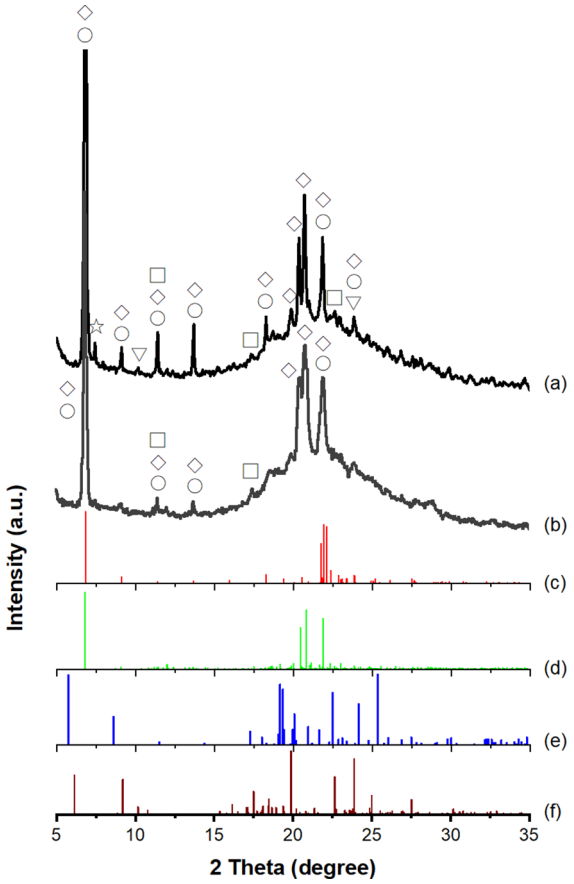

Figure 1. PXRD patterns of two purchased SDS: (a) Lot STBH5693 and (b) Lot MKBX0092V (labeled as "anhydrous") and theoretical patterns of (c) anhydrous SDS, (d) 1/8 hydrate, (e) hemihydrate, and (f) monohydrate from the Cambridge Crystallographic Data Centre (CCDC). The symbols assigned were as follows: circle, anhydrous SDS; diamond, SDS·1/8 hydrate; square, SDS·hemihydrate; inverted triangle, SDS·monohydrate; and star, unknown.

from the slurry with high viscosity very difficult and energy-consuming. On such basis, spray drying is advantageous for the direct removal of water in the production of SDS as compared to conventional evaporative crystallization or concentration under reduced pressure.

To the best of our knowledge, most of the studies on SDS crystallization were carried out by cooling in aqueous solutions below its critical micelle temperature. Although we have successfully produced SDS crystals reproducibly of a single hydrate form that is 1/8 hydrate by a series of operations,[25] there is no other study on the use of organic solvents for the hydrate screening of SDS. Therefore, in the present study, we started to screen for other new SDS hydrate form(s) with 19 common solvents for the very first time.

The form space of SDS in Table S1 displays five good solvents that give a solubility power of ≥5 mg/mL. They are DMF, ethanol, DMSO, methanol, and water. When water is chosen as a good solvent, THF, acetone, 1,4-dioxane, IPA, or ACN may serve as an antisolvent to precipitate SDS solids. Thus, the five water-miscible solvents—THF, acetone, 1,4-dioxane, IPA, and ACN—were individually added to a 20 wt % SDS aqueous solution (aq). Two common methods—antisolvent addition and temperature cooling—were attempted to induce SDS crystallization and to attain a high-quality product. No matter which antisolvent was added to the 20 wt % SDS (aq), there were no SDS solids being produced even up to a volume ratio of 1:10 (v/v). Apparently, antisolvent crystallization could not be employed for the 20 wt % SDS (aq) with those solvents in our cases. The other method, cooling crystallization, was also conducted by preparing the mixed solutions consisting of a 20 wt % SDS (aq) and one of the five solvents at a volume ratio of 1:3 and then by cooling those solutions from 25 to 4−6 °C. Only two of the resulting solutions with acetone and ACN gave thin plate- and needle-shaped crystals of SDS, respectively. The needle-shaped SDS crystals were determined to be a novel hydrate form based on its PXRD pattern that is distinct from all known SDS structures. PXRD is the most reliable and widely employed technique to identify polymorphs, hydrates, and solvates. A mixture of thin plate and needle crystals was produced from the resulting solution with ACN at the ratio of 1:4 (v/v). When the ratio went up to 1:5 (v/v), almost all crystals produced were thin plates, pointing to SDS·1/8 hydrate. A 33 wt % SDS (aq) was also used. Accordingly, only the 1:3 ratio of 20 or 33 wt % SDS (aq) to ACN is able to generate the purely specific novel hydrate form of SDS.

Although we did not have the other SDS hydrate forms at hand, including the hemi-, mono-, and dihydrate, as well as their solid-state characterizations, the theoretical patterns of those SDS hydrate forms were treated as standards for comparisons. An attempt was made to grow a single crystal of the novel SDS hydrate form for its structural determination by single crystal X-ray diffraction by SXD. Unfortunately, the decay of diffraction intensities for the single crystal was observed upon X-ray shining due to its amorphization.[22,23] This mishap had made data collection difficult and resulted in the incomplete structural refinement of the novel hydrate form. Based on our preliminary SXD data, the novel hydrate form was considered a form of tetrahydrate, having a stoichiometric ratio of SDS to water of 1:4 in the crystal lattice. The PXRD pattern of the novel SDS hydrate matches well with its theoretical pattern generated from SXD data (Figure 2) and shows a characteristic peak at $2\theta \approx 7.5°$. This characteristic peak is responsible for the unknown peak that exists in the PXRD pattern of one of the purchased SDS products (Figure 1a). Another peak at $2\theta \approx 6.8°$ is also notable for the novel

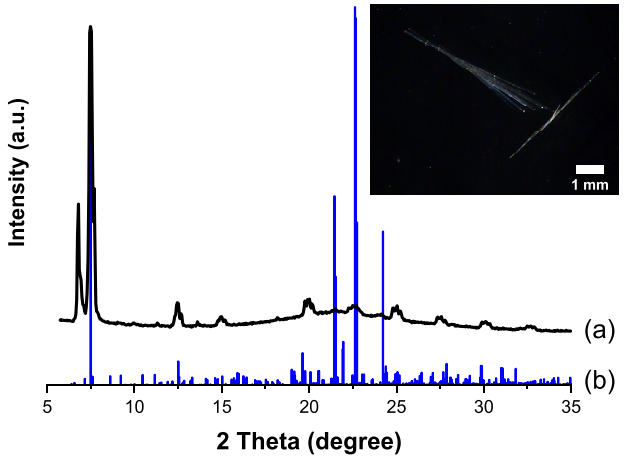

Figure 2. (a) PXRD pattern and (b) theoretical pattern of the novel SDS hydrate produced by recrystallization with a 1:3 (v/v) ratio of 20 wt % SDS to ACN, including its optical microscopy (OM) image (inset).

https://doi.org/10.1021/acsomega.1c01147
ACS Omega 2021, 6, 15770−15781

Table 1. Crystallographic Data for All the Resolved SDS Structures/Forms

	1/8 hydrate	hemihydrate	monohydrate	the novel hydrate	anhydrous
crystal habit	thin plate	plate	prism	needle	N/A
crystal system	monoclinic	monoclinic	triclinic	triclinic	monoclinic
space group	$C2/c$	$C2$	$P\bar{1}$	$P\bar{1}$	$P2_1/c$
a (Å)	78.69 (26)	9.847 (1)	10.423 (4)	9.334 (3)	38.9150
b (Å)	10.220 (22)	5.248 (1)	5.662 (3)	13.922 (5)	4.7090
c (Å)	16.410 (45)	30.798 (6)	28.913 (12)	35.652 (13)	8.1980
α (°)			86.70 (4)	97.342 (5)	
β (°)	98.28 (8)	91.29 (1)	93.44 (4)	90.385 (7)	93.2900
γ (°)			89.55 (4)	90.040 (5)	
density (g/cm^3) (calculated)	1.07893	1.23716	1.18899	1.14781	1.27707
ref	[21]	[22]	[23]	this study	[24]

SDS hydrate (Figure 2a). Also, three strong peaks at $2\theta \approx 21.5$, 22.7, and 24.2° are found in the theoretical pattern (Figure 2b), yet the relative intensities of those peaks are quite different from the ones in the PXRD pattern (Figure 2a). In addition to a structural factor, other factors and parameters, such as temperature, absorption, defects, strains, and size of a powdered sample, could lead to the difference in positions, widths, and relative intensities of diffraction peaks.[40] Crystallographic data for those reported SDS structures, including crystal systems, space groups, and lattice constants, were collected in Table 1 for comparison purposes. Such data are dissimilar to each other, confirming the formation of a novel SDS hydrate form that crystallizes in a triclinic crystal system.

To verify our hypothesis that the novel hydrate is tetrahydrate, TGA was used to measure the weight loss upon dehydration by heating and to calculate the stoichiometric ratio of SDS to water in Figure 3. After sample weighing, the

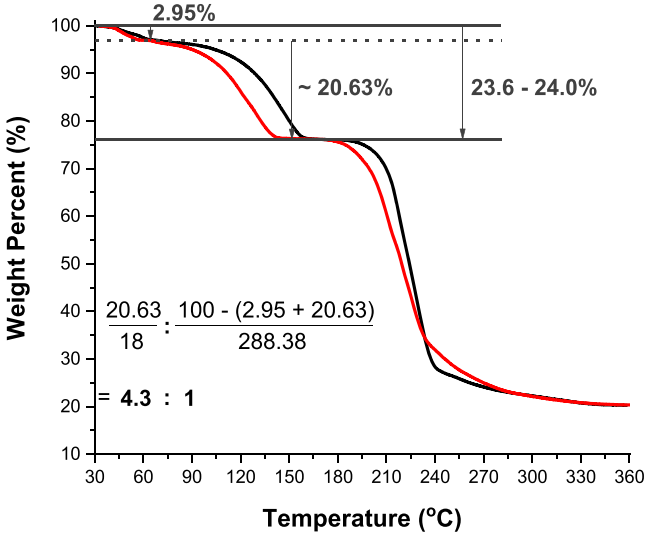

Figure 3. TGA scans of the novel SDS hydrate produced by recrystallization from two of our repeated experiments.

weight of the novel SDS hydrate started to decrease upon heating even at a low temperature range from 30° to around 70 °C with a weight loss of ~2.95%. A relatively flat curve of weight loss was then noticed over the temperature range of 70 to 90 °C. Afterward, there is another clear-cut weight loss that amounts to about 20.63% prior to 150 °C in Figure 3 due to its dehydration. The first weight loss (i.e., ~2.95%) was considered to arise from some moisture being adsorbed onto the surface of the novel hydrate or existing nonstoichiometric hydrate(s) that can vary in the water content without a significant change in its crystal structure. Upon dehydration, water in the channel or open structural voids of nonstoichiometric hydrates will be removed at relatively lower temperatures.[41] In comparison, stoichiometric hydrates have a well-defined water content. The amount of the second weight loss (i.e., 20.63%) corresponds to 4.3 water molecules per SDS (i.e., 4.3 hydrate). Despite the variations in the weight loss, curve slope, and dehydration temperature in Figure 3, the TGA results can still support the formation of the SDS·tetrahydrate according to our preliminary SXD data. Ideally, the SDS hydrate forms, such as 1/8 hydrate, hemihydrate, monohydrate, dihydrate and "tetrahydrate", exhibit weight losses of 0.77, 3.03, 5.88, 11.10, and 19.98% upon dehydration, respectively. As a consequence, it is impossible to attain such a high weight loss (about 20%) by solely mixing any of the already known SDS hydrates, which possess much lower water contents than 20%, upon dehydration by heating.

The FTIR spectra in Figure S2b,c show two pure hydrate forms of SDS, 1/8 hydrate and the novel hydrate, respectively. As compared with the result of the PXRD pattern in Figure 1a, it was found that FTIR spectroscopy has difficulty in detecting the little proportion of other hydrates present in the purchased SDS product (Figure S2a,b). Although FTIR is unlikely to distinguish the pure SDS·1/8 hydrate from the other forms clearly, the pure novel hydrate form certainly shows a different FTIR spectrum (Figure S2c). As methyl vibrational bands for micellar slurry or coagels and crystalline hydrate forms are comparable,[32] all characteristic peaks at 1618, 1257, 1225, 1188, 1099, 1078, 1061, and 996 cm^{-1} for the novel hydrate were labeled by asterisks in Figure S2c. As compared to SDS·1/8 hydrate (Figure S2b), no distinct peak is observed in the C−H stretching region of 3100−2800 cm^{-1}. The small band at 1618 cm^{-1} could be assigned to the bound water.[32] For the sulfate group (OSO_3^-) of SDS, the stretching bands are located at 1220 and 1084 cm^{-1} for 1/8 hydrate and 1225 and 1078 cm^{-1} for the novel hydrate form, which of the bands at 1225 cm^{-1} has also been noticed for dihydrate in the literature.[32] Although the other bands seem to be unresolved yet, they are quite different from the ones for SDS·hemihydrate-, and SDS·monohydrate-containing slurries reported.

Since the characterization of Raman spectroscopy will not be significantly interfered with water, it was put to use to examine the novel SDS hydrate form as well. The moiety of SDS molecule remains intact as indicated in Figure 4. There was no undesired reaction taking place to give other species or any

https://doi.org/10.1021/acsomega.1c01147
ACS Omega 2021, 6, 15770−15781

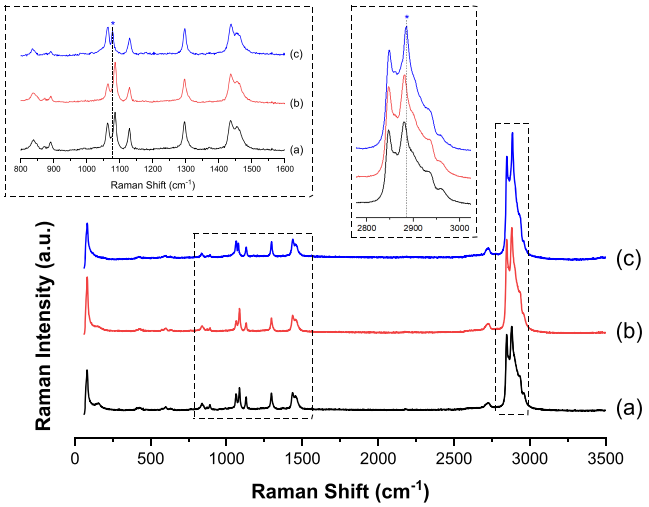

Figure 4. Raman spectra of the (a) purchased SDS, (b) SDS·1/8 hydrate, and (c) novel SDS hydrate.

impurities. All Raman assignments for SDS·1/8 hydrate are provided in Table 2.[31,42] The different hydrate forms of SDS

Table 2. Raman Assignments for SDS and SS

Raman shift (cm^{-1})	functional group	ref
	For SDS·1/8 hydrate	
2848, 2885	C−H stretching	[42]
1460, 1446	CH_2 bending	
1300	CH_2 twisting	
1130, 1078, 1062	C−C stretching	
890	$-CH_3$ rocking	
836	S−OC asymmetric stretching	
	For SS	
1102, 1132, 1152	SO_4 anti-symmetric stretching	[43]
993	SO_4 symmetric stretching	
622, 650	SO_4 bending	
453, 470	SO_4 bending	

display almost the same spectra in Figure 4, except the bands for C−H and C−C stretching, which are positioned at 2881 and 1085 cm^{-1} for the novel SDS hydrate, respectively.

The water sorption isotherms of the purchased SDS, SDS·1/8 hydrate, and novel SDS hydrate were analyzed by DVS at 25 °C and shown in Figure 5. Initially, the samples were dried at 0% RH to establish an equilibrium dry mass. As shown in Figure 5a, the pure SDS·1/8 hydrate looks very stable compared to the other two SDS samples for achieving the equilibrium in much shorter times at all conditions of different RHs. This reveals that SDS·1/8 hydrate can remain stable without increasing or losing its water content at all RH conditions. As verified, the dried weight of the pure 1/8 hydrate did not change at all (<0.15%) upon either sorption (i.e., RH up) or desorption (i.e., RH down) in Figure 5b. In other words, the plot of % RH *vs* elapsed time for achieving equilibrium in Figure 5a can tell whether a material can reach an equilibrium state at a certain RH condition within a given time (i.e., 4 h) or not for reference. The maximum time for equilibrium was set at 4 h in the present study. If the weight of a sample is still changing at a set RH condition and cannot find its equilibrium within 4 h, the sample still has to proceed to the next RH condition.

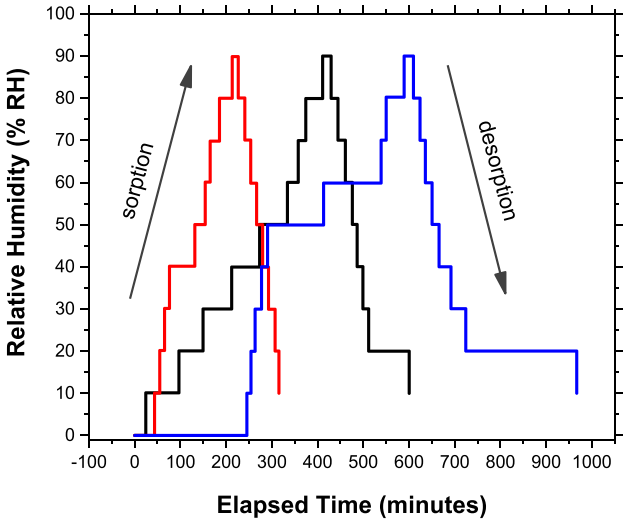

(a)

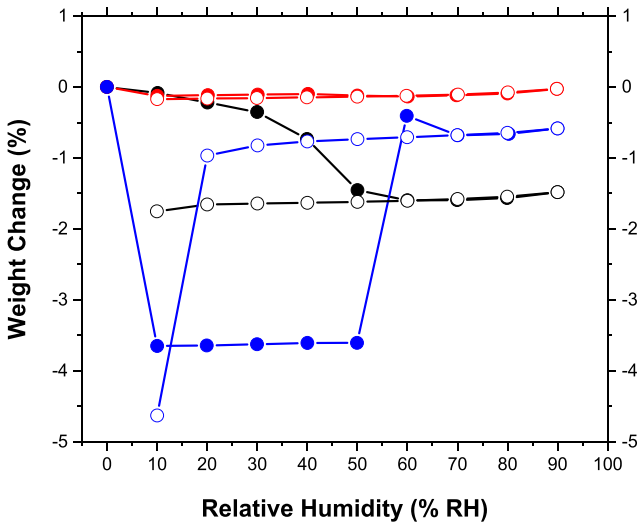

(b)

Figure 5. DVS isotherm plots of (a) % RH *vs* elapsed time and (b) weight change *vs* % RH of the purchased SDS (black), SDS·1/8 hydrate (red), and novel SDS hydrate (blue). Sorption isotherms were represented by solid circles, and desorption isotherms were represented by open circles.

The initial dried weight of the purchased SDS started to drop a bit by 1.7% over the range of 20 to 60% RH upon sorption by increasing % RH, and such loss is irreversible upon desorption by decreasing % RH. It indicates that either free moisture around the purchased SDS was removed or unstable hydrate(s) present in the purchased SDS had lost its hydrate content and transformed into the stable 1/8 hydrate, while the purchased SDS is considered as a mixture of different hydrate forms based on the PXRD pattern in Figure 1a.

Therefore, unlike the 1/8 hydrate, the weight loss of the purchased SDS could not be regained upon desorption, causing its weight change curves un-overlapped upon sorption and desorption. On the other hand, the novel hydrate form is

https://doi.org/10.1021/acsomega.1c01147
ACS Omega 2021, 6, 15770−15781

Scheme 1. Synthesis of SDS, including Sulfonation and Saponification

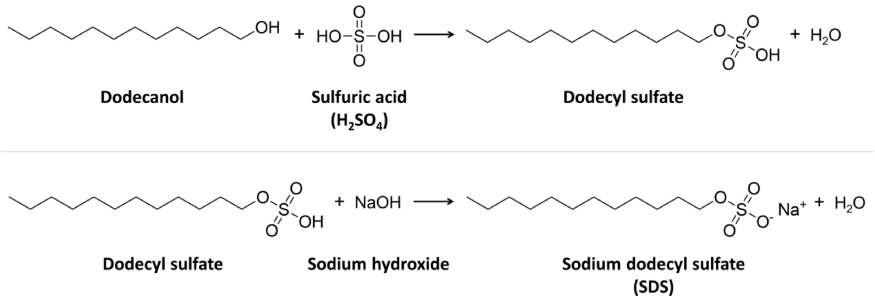

comparatively unstable, which could not reach equilibrium at the very low 0% RH in 4 h (i.e., 240 min) (Figure 5a). Consequently, the initial dried weight of the novel hydrate was not in equilibrium, and thus, it sharply dropped by 3.6% upon sorption from 0 to 10% RH (Figure 5b). This is in agreement with the TGA results (Figure 3) that ∼3% of the weight loss due to the presence of nonstoichiometric hydrate(s) was dehydrated by heating or at very low % RHs. Then, the weight of the novel hydrate remained relatively stable over the range of 10 to 50% RH and returned to −0.65% at 60% RH possibly because part of the free moisture or nonstoichiometric hydrate(s) was readsorbed. All three samples were quite stable at high RH above 70%. However, the novel hydrate was nearly unchanged upon desorption until a sudden drop in relative humidity to 10% RH. Some free moisture or nonstoichiometric hydrate(s) that was weakly bonded to SDS seemed to be desorbed from the novel hydrate, leading to the instability at low RH.

As suggested, EA was conducted to analyze the solid compositions of the SDS·1/8 hydrate and novel hydrate. EA results show that the elemental compositions of the SDS·1/8 hydrate by weight are as follows: 0 N% (nitrogen %), 49.48 ± 0.02 C% (carbon %), 10.29 ± 0.49 S% (sulfur %), 8.66 ± 0.34 H% (hydrogen %), and 23.75 ± 1.69 O% (oxygen %). Even though the data's reproducibility is not quite good for sulfur and oxygen %, it basically agrees to the chemical formula of SDS·1/8 hydrate that is $NaC_{12}H_{25}SO_4 \cdot 1/8\ H_2O$. However, the elemental compositions of the novel SDS hydrate are as follows: 0 N% (nitrogen %), 53.58 ± 0.15 C% (carbon %), 8.23 ± 0.23 S% (sulfur %), 10.39 ± 0.05 H% (hydrogen %), and 22.45 ± 0.23 O% (oxygen %), which are elusive and could not be related to the chemical formula of $NaC_{12}H_{25}SO_4 \cdot 4\ H_2O$. Only the hydrogen and sulfur % for the novel SDS hydrate are close to ones in the chemical formula. Consequently, more attempts to determine the crystal structure of the novel hydrate form by SXD as well as the interrelationships among the different hydrate forms of SDS will be made in the near future.

Preparation of the Novel SDS Hydrate from Chemical Synthesis. Following the preparation and solid-state characterizations of the pure novel SDS hydrate, a crystallization process was further developed by connecting with the chemical synthesis of SDS. In the process, SDS was synthesized by sulfonation of dodecanol with H_2SO_4 and subsequent saponification with NaOH (Scheme 1).[44] According to a general experimental procedure, SDS can be rapidly precipitated out at ambient temperature by adding sodium chloride (NaCl) (aq).[45] It is known as salting out. In that case, Na^+ and Cl^- ions in the solution will bind to polar water molecules and help separate the water molecules from SDS that cause the reduced solubility based on the common ion effect.[46] Large lumps of SDS crystals were then formed, filtered, and rinsed with ice water.

To avoid the addition of NaCl for salting out as well as the uncontrolled precipitation, two common crystallization methods, cooling and antisolvent addition, were introduced to develop a crystallization process of making the novel SDS hydrate in the present study. Sulfonation, also called esterification, by reacting dodecanol with H_2SO_4 (aq), was carried out at 75 °C to form dodecyl sulfate. Sulfuric acid plays the role of a catalyst to speed up the reaction and to force the equilibrium to the right-hand side of the reaction in Scheme 1 with a greater yield, and also acts as a dehydrating agent.[47,48] Therefore, an excess amount of sulfuric acid was added. Since the esterification reaction is exothermic, sulfuric acid (aq) was added slowly to prevent undesirable decomposition. Dodecyl sulfate was then converted into SDS by saponification using NaOH (aq). The reaction solution started to precipitate out during the addition of NaOH (aq) and formed a thick slurry after completion of the addition. The slurry was composed of micelles, liquid crystals, and coagels. However, the residual sulfuric acid would react with part of NaOH through neutralization to give unwanted sodium sulfate (SS) in a side reaction. The saturated concentration of SDS (i.e., solubility) would be lowered in the presence of SS. It was measured that SDS could barely be dissolved in 8 wt % SS (aq), and its solubility decreases as the proportion of SS increases. When cooling from 75 to 25 °C, the slurry became much thicker, making the control of SDS crystallization through proper transport phenomena more complicated, while several phases, including micelles, liquid crystals, and coagels, occurred as shown in Figure 6a.

In addition, the side product, SS, is also highly soluble in water. Accordingly, it was difficult to separate SDS from SS in the aqueous reaction solution and to maximize the yield of SDS. For such a case, spray drying cannot be used to produce a purified SDS product directly from the reaction solution containing other components. A crude product of SDS should be redissolved and then purified in a separate recrystallization step or spray drying process.

However, in the present study, an organic solvent was selected to serve as an antisolvent for crystallizing out SS without causing the crystallization of SDS at the same time. In the form space of SS in Table S2, water is the only good solvent, while the others are all bad solvents for SS. Also, based on the screening results for SDS, ACN and acetone could possibly be utilized as an antisolvent and to start the SDS crystallization by cooling to around 5 °C. The other solvents failed to induce SDS crystallization by the same operations. Therefore, the two solvents (i.e., ACN and acetone) were

https://doi.org/10.1021/acsomega.1c01147
ACS Omega 2021, 6, 15770−15781

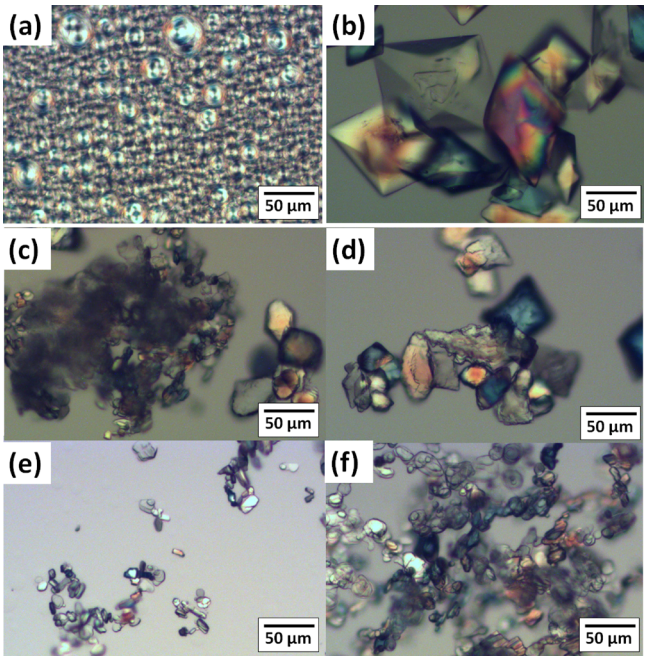

Figure 6. Polarized optical microscopy images of (a) the slurry at 25 °C after SDS synthesis; (b) SS crystals produced upon the addition of acetone at 25 °C; and SDS crystals during aging at 5 °C for (c) 2 h, (d) 4 h, (e) 6 h, and (f) 8 h.

chosen for the development of a crystallization process in the present study.

While ACN was added into the slurry (i.e., the aqueous reaction solution) after cooling it to 25 °C at a ratio of 1:1 (v/v), SS was crystallized out in the slurry also containing SDS precipitates. As a consequence, SS and SDS solids could not be separated from each other through the addition of ACN. On the contrary, the slurry was turning into a clear solution when acetone was introduced with a ratio of 1:1 (v/v). All SDS solids were then dissolved, but SS started to crystallize out instead. Moreover, the micellization of SDS can be inhibited by the addition of acetone as verified by DLS in Figure S3, which is the reason for dissolving of the slurry. At the CMC of SDS, the DLS scan shows a size distribution at around 2 nm owing to the formation of micelles (Figure S3a) in 8.2 mM SDS (aq). As for 20 wt % SDS (aq), two size distributions at 2 and 100 nm are observed, and the larger size distribution suggests the presence of micellar aggregates.[49,50] Upon the addition of acetone, the two peaks then vanished, implying that the structures of micelles and micellar aggregates of SDS have been destroyed.

As mentioned earlier, the saturated concentration of SDS increases in the absence of SS or after the crystallization of SS upon the addition of acetone. It implies that SDS and SS could be easily separated by the addition of acetone. The SS crystals produced, upon the addition of four times the volume of acetone to water, were isolated by cake filtration and oven drying at 40 °C. SDS remained dissolved in the filtrate (i.e., the mother liquor) where the solution composition was still undersaturated for SDS. Subsequently, SDS crystals of the novel hydrate form were successfully made by cooling the mother liquor from 25 to 5 °C. Those crystals were also collected by cake filtration and oven drying at 40 °C and characterized by PXRD.

Their solubility relationship in Figure 7 was illustrated by the solubility curves of SDS and SS in water−acetone solutions

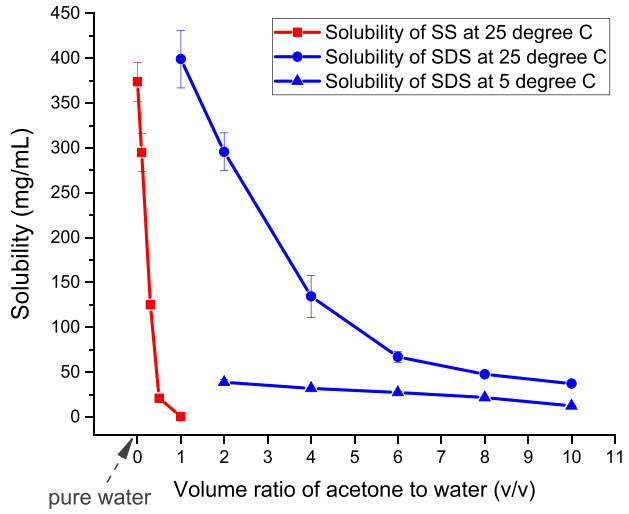

Figure 7. The solubility relationship between SS and SDS upon the addition of acetone. The solubility values of SS at 25 °C were represented by red solid squares, and the ones of SDS at 25 and 5 °C were represented by blue solid circles and triangles, respectively.

with various volume ratios to depict the individual crystallization pathways. The solubility value of SS in pure water was measured to be 373.5 ± 21.6 mg/mL at 25 °C. Upon the addition of acetone, the solubility of SS was drastically decreased as shown by the slant slope of its solubility curve in Figure 7. As acetone was added to a ratio of acetone to water of 0.5:1 (v/v), the solubility value would be lowered to 20.9 ± 2.3 mg/mL. Almost no SS solid can be dissolved in the 1:1 (v/v) solution at 25 °C. It reveals that acetone plays a proper role in the antisolvent crystallization of SS. In contrast with SS, SDS still has a quite high solubility value of 399.0 ± 32.2 mg/mL in the 1:1 (v/v) solution at 25 °C.

Therefore, by virtue of the great change in its solubility, SS could easily be isolated alone upon the addition of acetone. To facilitate the SS crystallization, acetone was added up to a ratio of 4:1 (v/v). For this process achieved in a 100 mL flask, about 1.25 g of pure SS was harvested and characterized by FTIR, Raman, and PXRD in Figures S4 to S6, respectively, to be an anhydrous form. Anhydrous SS crystals show a bipyramidal habit as illustrated in Figure 6b.

Since we did not have any access to an HPLC equipped with a charged aerosol detector (CAD) for SDS, the actual concentration of SDS was inferred based on the amount of anhydrous SS crystals produced. Besides, the complete composition for such a system was hard to be specified by Raman spectroscopy. Assuming a complete conversion rate for neutralization that residual or unreacted sulfuric acid would totally form SS with NaOH, the conversion rate into SDS was calculated to be 74%. Based on this calculation, 4.15 g of SDS would be produced to give an approximated initial concentration of 377.0 mg/mL in the slurry prior to the acetone addition (marked as a dark blue asterisk in Figure 8).

As double the volume of acetone was added, the slurry turned into a clear solution with a 1:1 (v/v) ratio of acetone to water due to the dissolution of SDS. Upon the first addition of acetone to the 1:1 (v/v) solution, the concentration of SDS

https://doi.org/10.1021/acsomega.1c01147
ACS Omega 2021, 6, 15770−15781

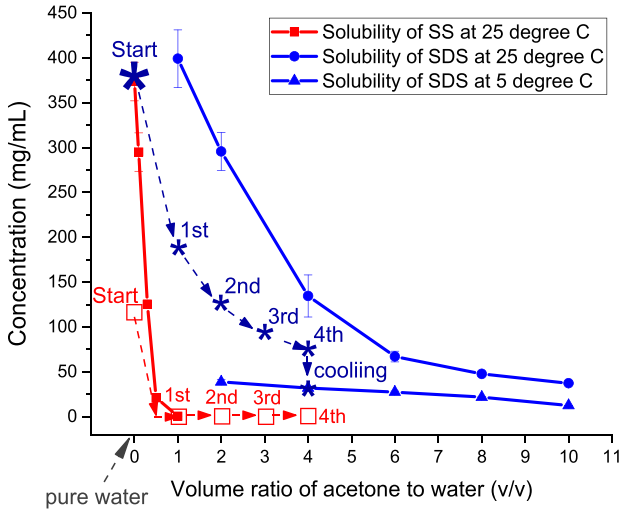

Figure 8. The crystallization pathways of anhydrous SS upon the four times addition of acetone depicted by red open squares and the novel SDS hydrate form upon four times addition of acetone and cooling depicted by dark blue asterisks based on their solubility curves established in Figure 7.

was reduced by two times to become 188.5 mg/mL at 25 °C. Until the solution was diluted by four times the volume of acetone to a 4:1 (v/v) solution (i.e., upon the fourth addition of acetone), SDS was still undersaturated in the solution with a concentration of 75.4 mg/mL in the 4:1 (v/v) solution at 25 °C. The resulting solution was then filtered to obtain SS crystals. Next, the mother liquor was poured into another stirred tank and cooled from 25 to 5 °C for crystallizing the novel SDS hydrate as depicted in Figure 8. Finally, 3.19 g of the novel SDS hydrate crystals was harvested by cake filtration and oven drying. The crystal yield was 61.5% as we hypothesized that the novel hydrate is a form of tetrahydrate.

Furthermore, this process was scaled up to a 0.5 L-sized stirred glass tank as shown in Figure 9. In general, the operation of crystallization is completed overnight or within 8−12 h. For large-scale production, it usually takes 6 to 8 h to discharge a 4000 L-sized vessel. To ensure that the novel SDS hydrate could be preserved without phase transformation during discharging, the time for its crystallization and aging at 5 °C was prolonged from 2 h in the round-bottom flask to 8 h in the stirred tank. The crystals produced by cooling were sampled for OM, FTIR, and PXRD at an interval of time of 2 h until a total of 8 h. Their size distribution became more uniform in size ranging from 15 to 50 μm during aging for 8 h as shown in Figure 6c−f. The needle-shaped crystals shown in the inserted OM image of Figure 2 were obtained through recrystallization by statically cooling in a refrigerator. The crystallization process, connecting with the synthesis of SDS, was carried out under agitation throughout to produce a plate-like crystal habit (Figure 6c−f). We speculate that the plate-like habit in the stirred tank could be due to a different solution medium/environment for crystallization, the breakage of needle crystals under stirring, and/or preferential crystal growth toward a definite plane or direction under fluid flow. It was evidenced by the evolution of the relative intensities of the first two peaks at 2θ = 6.8 and 7.5° in the PXRD pattern of Figure 10 during aging for 8 h, both of which are assigned to the novel SDS hydrate form in Figure 2. The intensity of the characteristic peak at 2θ = 7.5° for the novel hydrate becomes much stronger than the one at 6.8° as the aging time is

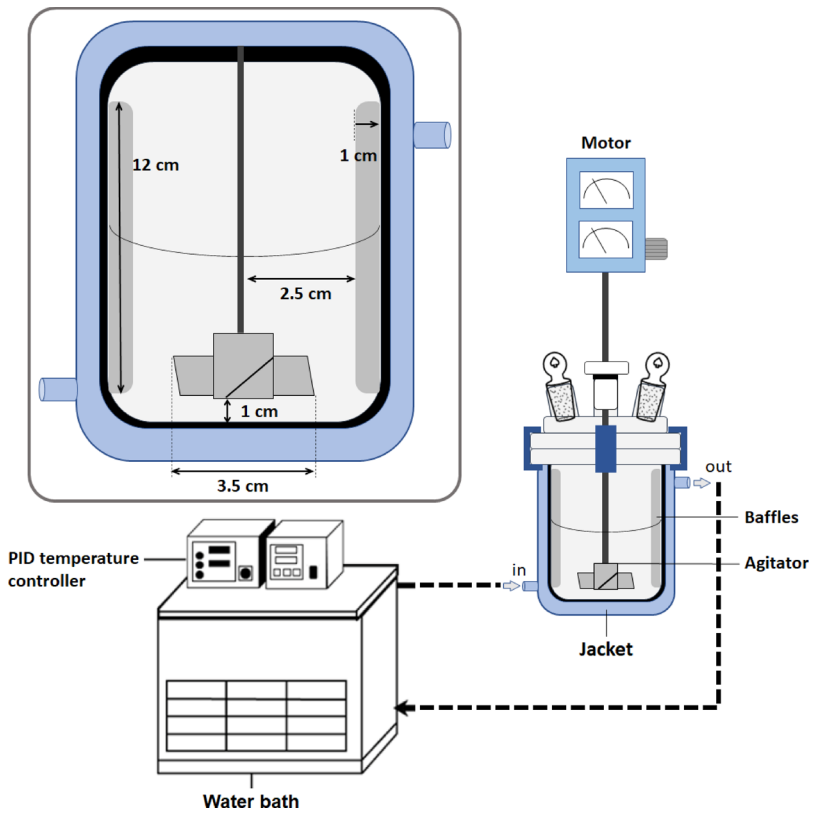

Figure 9. Configuration of the 0.5 L-sized jacketed glass tank used in the present study equipped with a temperature-controlled water bath.

https://doi.org/10.1021/acsomega.1c01147
ACS Omega 2021, 6, 15770−15781

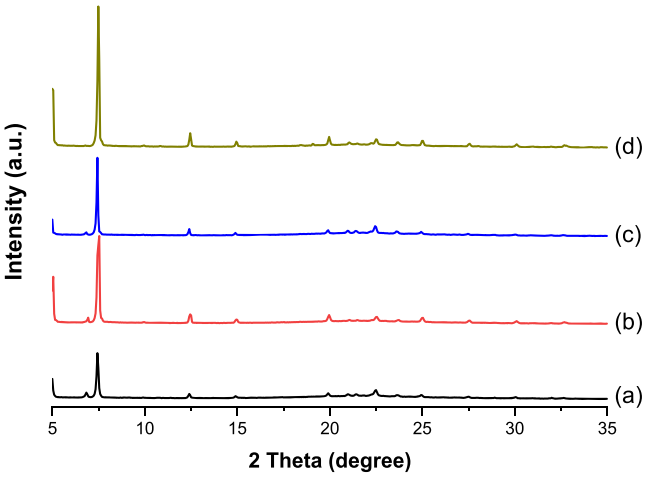

Figure 10. PXRD patterns of SDS crystals of the novel hydrate during aging at 5 °C for (a) 2 h, (b) 4 h, (c) 6 h, and (d) 8 h.

increased. The other peak at 2θ = 6.8° almost disappears. Therefore, the process of making the novel SDS hydrate was successfully scaled up.

CONCLUSIONS

Two purchased SDS products were verified to be a mixture of various hydrates of SDS. Apparently, there was an unknown hydrate form of SDS existing in one of the two purchased products. As a result, the hydrate screening of SDS was carried out with the use of organic solvents based on two common crystallization methods, including antisolvent addition and temperature cooling, for the very first time. While the crystallization of SDS could not be induced from a 20 wt % SDS (aq) solely upon the addition of different organic solvents even up to a volume ratio of 1:10, a novel SDS hydrate form was produced by coupling antisolvent addition with cooling from 25 to 5 °C. Needle-shaped crystals of the novel hydrate form were produced from a solution made of a 20 wt % SDS (aq) and ACN at a ratio of 1:3 (v/v), and characterized by PXRD, TGA, FTIR, Raman, DVS, and EA. Despite its incomplete structural refinement by SXD, the novel hydrate form was considered as a form of tetrahydrate. Furthermore, a crystallization process for the novel SDS hydrate was developed linking the two-stage chemical synthesis of sulfonation and saponification of SDS. Such process was also successfully scaled up to be operated in a 0.5 L-sized stirred tank. Plate-like crystals of the novel hydrate form were produced in the stirred tank and would not transform during aging for 8 h at 5 °C.

EXPERIMENTAL DETAILS

Materials. Sodium dodecyl sulfate (SDS) ($C_{12}H_{25}NaO_4S$, MW 288.38 g/mol, ≥99.0% purity, Lot STBH5693 for SDS pellets, and Lot MKBX0092V for anhydrous SDS powder) was purchased from Sigma-Aldrich (China). 1-Dodecanol ($C_{12}H_{26}O$, MW 186.34 g/mol, >99.0% purity, Lot OREBD-JO) was obtained from Tokyo Chemical Industry (TCI) Co., Ltd. (Japan). Sulfuric acid (H_2SO_4, MW 98.08 g/mol, >97% assay, Lot 0C397) and sodium hydroxide (NaOH, MW 40.00 g/mol, >97.0% assay, Lot KBB-055C) were received from Showa (Japan). Anhydrous sodium sulfate (SS) (Na_2SO_4, MW 142.04 g/mol, >99.0% assay, Lot 62290) was received from Riedel-de Haën (Germany).

Form Space Establishment. Five milligrams of the purchased SDS or sodium sulfate (SS) solids was weighed into a scintillation vial, and 1 mL of the solvent was titrated into the vial at 25 °C with intermittent shaking. Nineteen common solvents were screened by an initial solvent screening method developed by Lee et al.[51] Those solvents include *n*-heptane, ethyl acetate, toluene, methyl *tert*-butyl ether, methyl ethyl ketone, chloroform, tetrahydrofuran, dimethylaniline, acetone, 1,4-dioxane, 1-butanol, isopropyl alcohol, benzyl alcohol, acetonitrile (ACN), dimethylformamide, ethanol, dimethyl sulfoxide, methanol, and water.

Solubility Measurement. Stock solutions of water and acetone were prepared at different volume ratios of 1:0.1, 1:0.3, 1:0.5, 1:1, 1:2, 1:4, 1:6, and 1:8 (v/v). The gravimetric method was used to measure the solubility values of SS in the prepared stock solutions with the ratios of 1:0.1, 1:0.3, 1:0.5, and 1:1 (v/v) and the ones of SDS in the prepared stock solutions with the other ratios of 1:1, 1:2, 1:4, 1:6, and 1:8 (v/v). A specified quantity of the purchased SDS or SS solids was weighted into a scintillation vial, which had been warmed up in a temperature-controlled water bath. Each solution was titrated very slowly into the vial with intermittent shaking until all solids were just dissolved. The solubility measurement was carried out carefully at 5 and 25 °C for 3 days and repeated three times.

Preparation of a Novel SDS Hydrate by Recrystallization. A 20 wt % SDS aqueous stock solution (aq) was prepared. Three milliliters of the 20 wt % SDS (aq) was withdrawn into a scintillation vial, and 9 mL of ACN was then added with a ratio of 1:3 (v/v) at 25 °C. The resulting solution first became slightly turbid and then clear after shaking for several minutes. Shortly, it was placed in a refrigerator at 4−8 °C. Needle-shaped crystals were formed a few hours later and then filtered and air dried.

Crystallization Process of a Novel SDS Hydrate. A total of 6.73 mL of 1-dodecanol (0.03 mol) was first introduced in a 100 mL round-bottom flask at 75 °C. A total of 2.35 mL of ∼77 wt % H_2SO_4 (aq) (0.031 mol) was slowly added into the flask to react with 1-dodecanol by esterification for 2 h under magnetic stirring. The fast addition rate should be avoided for undesired decomposition. A total of 10.67 mL of 3 M NaOH (aq) (0.032 mol) was used to convert dodecyl sulfate, which was formed by the esterification, into SDS at the same temperature for 2 h. Later, the reaction solution was cooled from 75 to 25 °C in 1 h and turned into a highly concentrated slurry during cooling. Sampling was carried out at this time for solid-state characterizations, including polarized optical microscopy (OM), Fourier transform infrared (FTIR) spectroscopy, and powder X-ray diffraction (PXRD). Forty-four milliliters of acetone, which is about four times the volume of water (i.e., aqueous phase) in the reaction solution, was divided into four proportions. Each proportion was added into the reaction solution at an interval of 5 min. Most of the slurry or solid cake was dissolved soon when the first proportion of acetone was being fed at 25 °C. Adding the fourth proportion of acetone had prompted to make more crystals produced from the resulting solution, and after stirring for 2 h, it was filtered off. The solids on the filter paper with a pore size of 5 μm were oven dried at 40 °C and collected for OM, FTIR, Raman spectroscopy, PXRD, and thermogravimetric analysis (TGA). The filtrate (i.e., mother liquor) was subject to cooling crystallization from 25 to 5 °C in another flask for 2 h. The SDS crystals were then produced in

https://doi.org/10.1021/acsomega.1c01147
ACS Omega 2021, 6, 15770−15781

the mother liquor, collected by cake filtration and oven drying at 40 °C, and fully characterized.

To scale up this process, a 0.5 L jacketed glass tank was used in which a vertical agitator with a four-bladed impeller and four vertical baffles were installed. Teflon was coated on the agitator and baffles to prevent metal ion leaching, especially upon the addition of a high concentration H_2SO_4 (aq). Dimensions of the whole vessel were illustrated in Figure 10. Twelve milliliters of ∼77 wt % H_2SO_4 (aq) (0.14 mol) was added next to the impeller at a slow rate of 2 mL/min to mix with 30 mL of 1-dodecanol (0.134 mol), precharged in the tank at 75 °C, for 2 h. A total of 48.7 mL of 3 M NaOH (aq) (0.146 mol) was added at a faster rate of 10 mL/min to produce SDS at the same temperature for 2 h. As followed by cooling from 75 to 25 °C in 1 h, 200 mL of acetone that is approximately four times the volume of water in the reaction solution was introduced in four proportions. The resulting solution was kept at 25 °C under agitation for 8 h and filtered off to collect SS crystals. The mother liquor after filtration was transferred to another 0.5 L jacketed glass tank at 25 °C, and subsequently, it was cooled to 5 °C for SDS crystallization and aged for 8 h. During this period, the solution was sampled every 2 h. Finally, the SDS crystals were harvested by cake filtration and oven drying at 40 °C and then characterized by OM, FTIR, and PXRD.

Instrumental Analysis. Polarized optical microscopy (OM) (Olympus SZII Zoom Stereo, Tokyo, Japan) with a charge-couple device (CCD) camera was used to observe particle size and morphology. PXRD diffraction (Bruker D8 Advance, Karlsruhe, Germany) using Cu Kα radiation (λ = 1.5418 Å) was used for phase identification. The diffractometer was operated at 40 keV and 40 mA to generate diffraction patterns at a scanning rate of 2° 2θ/min from 5 to 35°. TGA (Perkin Elmer Pyris 1, Norwalk, CT, USA) was used to measure the weight loss of a sample as a function of temperature, possibly due to dehydration or desolvation, decomposition, or sublimation. Samples placed in a Pt pan suspended open in a furnace were heated from 30 to 350 °C at a heating rate of 10 °C/min under a nitrogen atmosphere. FTIR spectroscopy (Perkin Elmer Spectrum One, Shelton, CT, USA) was used to identify organic and polymeric compounds. Each solid sample was ground with KBr powder to form a tablet using a hydraulic hand press under 7.5 tons, which was scanned in the region of 4000 to 400 cm^{-1} eight times with a resolution of 2 cm^{-1}. Raman spectroscopy was used to determine vibrational modes and to measure the chemical composition of a solid sample. Raman spectra in the range of 60 to 3500 cm^{-1} were acquired with an exposure time of 10 s for eight scans using a green laser at 532 nm, whose actual laser energy through an objective lens was 5 to 30 mW. A silicon substrate (SiO_2/Si) (4 in. P-type (100) silicon wafer) was used for calibration to have a characteristic signal at 520 cm^{-1}. Dynamic vapor sorption (DVS) (TA Instruments VTI-SA+, New Castle, DE, USA) was used to determine water sorption isotherms at 25 ± 0.1 °C. Each solid sample was loaded into a symmetrical microbalance system (weighing precision: 0.01%) and dried at 0% relative humidity (RH) to establish an equilibrium dry mass initially. The sample was then exposed to environments of different RH ranging from 0 to 90% RH with an increment of 10% RH. The equilibrium criterion for jumping to the next % RH is the mass change of <0.001% for 5 min. The maximum equilibrium time for every condition was set at 240 min (i.e., 4 h). Elemental analysis (EA) (Elementar Heraeus Vario EL-III cube, Germany) was used for the weight content determination of nitrogen (N%), carbon (C%), sulfur (S%), hydrogen (H%), and oxygen (O%). Sulfanilic acid (N%: 8.09, C%: 41.55−41.61, S%: 18.51, and H %: 4.04−4.07) was used as a standard for the analysis of elements of N, C, S, and H. On the other hand, benzoic acid (O%: 26.22) was used as another standard for the analysis of element of O. The accuracy of the EA instrument is ±0.1%, precision is ±0.2%, and inaccuracy is ±0.3%. Dynamic light scattering (DLS) (Horiba SZ-100, Kyoto, Japan) was used to determine particle size distribution(s) in a solution phase.

■ ASSOCIATED CONTENT

Supporting Information

The Supporting Information is available free of charge at https://pubs.acs.org/doi/10.1021/acsomega.1c01147.

Form spaces of SDS and SS; TGA scans and FTIR spectra of the purchased SDS, SDS·1/8 hydrate, and novel SDS hydrate; DLS scans of 20 wt % SDS (aq)-acetone solutions; and FTIR, Raman, and PXRD of SS as supplied (PDF)

■ AUTHOR INFORMATION

Corresponding Author

Tu Lee − *Department of Chemical and Materials Engineering, National Central University, Taoyuan City 32001, Taiwan R.O.C.*; orcid.org/0000-0003-1846-3970; Phone: +886-3-4227151; Email: tulee@cc.ncu.edu.tw; Fax: +886-3-4252296

Authors

Hung Lin Lee − *Department of Chemical and Materials Engineering, National Central University, Taoyuan City 32001, Taiwan R.O.C.*; orcid.org/0000-0001-9931-8083

Yun Sheng Cheng − *Department of Chemical and Materials Engineering, National Central University, Taoyuan City 32001, Taiwan R.O.C.*

Kuan Lin Yeh − *Department of Chemical and Materials Engineering, National Central University, Taoyuan City 32001, Taiwan R.O.C.*

Complete contact information is available at: https://pubs.acs.org/10.1021/acsomega.1c01147

Notes

The authors declare no competing financial interest.

■ ACKNOWLEDGMENTS

This research was supported by grants from the Ministry of Science and Technology of Taiwan R.O.C. (MOST 107-2221-E-008-037-MY3 and 108-2731-M-008-001). We are indebted to the Precision Instrument Center at National Central University (NCU) for technical support. We also thank Ting-Shen Kuo for SXD measurement at National Taiwan Normal University, Dr. Hsin-Kuan Liu for informative discussion about our preliminary SXD data at NCU (currently at National Cheng Kung University), Ching-Wei Lu for EA measurement at National Taiwan University, and Dr. Jaydip M. Vasoya for DVS measurement at St. John's University, USA.

REFERENCES

(1) Schägger, H. Tricine-SDS-PAGE. *Nat. Protoc.* **2006**, *1*, 16−22.
(2) Deo, N.; Somasundaran, P. Effects of Sodium Dodecyl Sulfate on Mixed Liposome Solubilization. *Langmuir* **2003**, *19*, 7271−7275.
(3) Alizadeh, M. N.; Shayanfar, A.; Jouyban, A. Solubilization of Drugs Using Sodium Lauryl Sulfate: Experimental Data and Modeling. *J. Mol. Liq.* **2018**, *268*, 410−414.
(4) Vinarov, Z.; Katev, V.; Radeva, D.; Tcholakova, S.; Denkov, N. D. Micellar Solubilization of Poorly Water-Soluble Drugs: Effect of Surfactant and Solubilizate Molecular Structure. *Drug Dev. Ind. Pharm.* **2018**, *44*, 677−686.
(5) Xu, J.; Mueller, R.; Hazelbaker, E.; Zhao, Y.; Bonzongo, J. C. J.; Clar, J. G.; Vasenkov, S.; Ziegler, K. J. Strongly Bound Sodium Dodecyl Sulfate Surrounding Single-Wall Carbon Nanotubes. *Langmuir* **2017**, *33*, 5006−5014.
(6) Lee, Y. J.; Huang, L.; Wang, H.; Sushko, M. L.; Schwenzer, B.; Aksay, I. A.; Liu, J. Structural Rearrangement and Dispersion of Functionalized Graphene Sheets in Aqueous Solutions. *Colloids Interface Sci. Commun.* **2015**, *8*, 1−5.
(7) Kumar, A.; Bhattacharjee, G.; Kulkarni, B. D.; Kumar, R. Role of Surfactants in Promoting Gas Hydrate Formation. *Ind. Eng. Chem. Res.* **2015**, *54*, 12217−12232.
(8) Choudhary, N.; Hande, V. R.; Roy, S.; Chakrabarty, S.; Kumar, R. Effect of Sodium Dodecyl Sulfate Surfactant on Methane Hydrate Formation: A Molecular Dynamics Study. *J. Phys. Chem. B* **2018**, *122*, 6536−6542.
(9) Huang, X.; Li, W.; Wang, M.; Tan, X.; Wang, Q.; Wang, C.; Zhang, M.; Yuan, J. A Facile Template Route to Periodic Mesoporous Organosilicas Nanospheres with Tubular Structure by Using Compressed CO2. *Sci. Rep.* **2017**, *7*, 45055.
(10) Ahmed, M. A.; Rhgigh, A. M.; Shakeel, F. Effect of Surfactants on the Crystal Properties and Dissolution Behavior of Aspirin. *Asian J. Res. Chem.* **2009**, *2*, 202−206.
(11) Ghane-Motlagh, R.; Fammels, J.; Danilewsky, A. N.; Pelz, U.; Woias, P. Effect of Surfactants on the Growth and Characterization of Triglycine Sulfate Crystals. *J. Cryst. Growth* **2021**, *563*, 126081.
(12) Lakshmi, V. M.; Chakravarthy, S. R.; Rajendran, A. G.; Thomas, C. R. Effect of Crystallization Parameters and Presence of Surfactant on Ammonium Perchlorate Crystal Characteristics. *Particul. Sci. Technol.* **2016**, *34*, 308−316.
(13) Lee, T.; Zhang, C. W. Dissolution Enhancement by Bio-Inspired Mesocrystals: The Study of Racemic (*R*,*S*)-(±)-Sodium Ibuprofen Dihydrate. *Pharm. Res.* **2008**, *25*, 1563−1571.
(14) Qazi, M. J.; Liefferink, R. W.; Schleogel, S. J.; Backus, E. H. G.; Bonn, D.; Shahidzadeh, N. Influence of Surfactants on Sodium Chloride Crystallization in Confinement. *Langmuir* **2017**, *33*, 4260−4268.
(15) Lee, T.; Lin, H. Y.; Lee, H. L. Engineering Reaction and Crystallization and the Impact on Filtration, Drying, and Dissolution Behaviors: The Study of Acetaminophen (Paracetamol) by In-Process Controls. *Org. Proc. Res. Dev.* **2013**, *17*, 1168−1178.
(16) Lee, H. L.; Lin, H. Y.; Lee, T. Large-Scale Crystallization of a Pure Metastable Polymorph by Reaction Coupling. *Org. Proc. Res. Dev.* **2014**, *18*, 539−545.
(17) Lee, H. L.; Chiu, C. W.; Lee, T. Engineering Terephthalic Acid Product from Recycling of PET Bottles Waste for Downstream Operations. *Chem. Eng. J. Adv.* **2021**, *5*, 100079.
(18) Chantraine, F.; Viana, M.; Cazalbou, S.; Brielles, N.; Mondain-Monval, O.; Pouget, C.; Branlard, P.; Rubinstenn, G.; Chulia, D. From Compressibility to Structural Investigation of Sodium Dodecyl Sulfate − Part 1: Powder and Tablet Physico-chemical Characteristics. *Powder Technol.* **2007**, *177*, 34−40.
(19) Smith, L. A.; Duncan, A.; Thomson, G. B.; Roberts, K. J.; Machin, D.; McLeod, G. Crystallization of Sodium Dodecyl Sulfate from Aqueous Solution: Phase Identification, Crystal Morphology, Surface Chemistry and Kinetic Interface Roughening. *J. Cryst. Growth* **2004**, *263*, 480−490.
(20) Lu, J.; Li, Z.; Jiang, X. Polymorphism of Pharmaceutical Molecules: Perspectives on Nucleation. *Front. Chem. Eng. China* **2010**, *4*, 37−44.
(21) Sundell, S. The Crystal Structure of Sodium Dodecylsulfate. *Acta Chem. Scand.* **1997**, *31*, 799−807.
(22) Coiro, V. M.; Mazza, F.; Pochetti, G. Crystal Phases Obtained from Aqueous Solutions of Sodium Dodecyl Sulfate. The Structure of a Monoclinic Phase of Sodium Dodecyl Sulfate Hemihydrate. *Acta Cryst. C* **1986**, *42*, 991−995.
(23) Coiro, V. M.; Manigrasso, M.; Mazza, F.; Pochetti, G. Structure of a Triclinic Phase of Sodium Dodecyl Sulfate Monohydrate. A Comparison with Other Sodium Dodecyl Sulfate Crystal Phases. *Acta Cryst. C* **1987**, *43*, 850−854.
(24) Smith, L. A.; Hammond, R. B.; Roberts, K. J.; Machin, D.; McLeod, G. Determination of the Crystal Structure of Anhydrous Sodium Dodecyl Sulphate Using a Combination of Synchrotron Radiation Powder Diffraction and Molecular Modelling. *J. Mol. Struct.* **2000**, *554*, 173−182.
(25) Lee, T.; Yeh, K. L.; You, J. X.; Fan, Y. C.; Cheng, Y. S.; Pratama, D. E. Reproducible Crystallization of Sodium Dodecyl Sulfate·1/8 Hydrate by Evaporation, Antisolvent Addition, and Cooling. *ACS Omega* **2020**, *5*, 1068−1079.
(26) Muramatsu, M.; Inoue, M. A Radiotracer Study on Slow Hydrolysis of Sodium Dodecylsulfate in Aqueous Solution. *J. Colloid Interface Sci.* **1976**, *55*, 80−84.
(27) Bethell, D.; Fessey, R. E.; Namwindwa, E.; Roberts, D. W. The Hydrolysis of C12 Primary Alkyl Sulfates in Concentrated Aqueous Solutions. Part 1. General Features, Kinetic Form and Mode of Catalysis in Sodium Dodecyl Sulfate Hydrolysis. *J. Chem. Soc., Perkin Trans. 2* **2001**, 1489−1495.
(28) Kékicheff, P.; Grabielle-Madelmont, C.; Ollivon, M. Phase Diagram of Sodium Dodecyl Sulfate-Water System: 1. A Calorimetric Study. *J. Colloid Interface Sci.* **1989**, *131*, 112−132.
(29) Kékicheff, P. Phase Diagram of Sodium Dodecyl Sulfate-Water System: 2. Complementary Isoplethal and Isothermal Phase Studies. *J. Colloid Interface Sci.* **1989**, *131*, 133−152.
(30) Fontell, K. Liquid Crystallinity in Lipid-Water Systems. *Mol. Cryst. Liq. Cryst.* **1981**, *63*, 59−82.
(31) Picquart, M. Vibrational Mode Behavior of SDS Aqueous Solutions Studied by Raman Scattering. *J. Phys. Chem.* **1986**, *90*, 243−250.
(32) Sperline, R. P. Infrared Spectroscopic Study of the Crystalline Phases of Sodium Dodecyl Sulfate. *Langmuir* **1997**, *13*, 3715−3726.
(33) Smith, L. A.; Roberts, K. J.; Machin, D.; McLeod, G. An Examination of the Solution Phase and Nucleation Properties of Sodium, Potassium and Rubidium Dodecyl Sulphates. *J. Cryst. Growth* **2001**, *226*, 158−167.
(34) Smith, L. A.; Thomson, G. B.; Roberts, K. J.; Machin, D.; McLeod, G. Modeling the Crystal Morphology of Alkali-Metal Alkyl Surfactants: Sodium and Rubidium Dodecyl Sulfates. *Cryst. Growth Des.* **2005**, *5*, 2164−2172.
(35) Miller, R. M.; Poulos, A. S.; Robles, E. S.; Brooks, N. J.; Ces, O.; Cabral, J. T. Isothermal Crystallization Kinetics of Sodium Dodecyl Sulfate-Water Micellar Solutions. *Cryst. Growth Des.* **2016**, *16*, 3379−3388.
(36) Miller, R. M.; Ces, O.; Brooks, N. J.; Robles, E. S. J.; Cabral, J. T. Crystallization of Sodium Dodecyl Sulfate-Water Micellar Solutions under Linear Cooling. *Cryst. Growth Des.* **2017**, *17*, 2428−2437.
(37) Khodaparast, S.; Marcos, J.; Sharratt, W. N.; Tyagi, G.; Cabral, J. T. Surface-Induced Crystallization of Sodium Dodecyl Sulfate (SDS) Micellar Solutions in Confinement. *Langmuir* **2021**, *37*, 230−239.
(38) Ramakers, H. P. E. Alkyl Sulphate Salts. US Patent 5147633A, 1992.
(39) Moroi, Y.; Motomura, K.; Matuura, R. The Critical Micelle Concentration of Sodium Dodecyl Sulfate-Bivalent Metal Dodecyl Sulfate Mixtures in Aqueous Solution. *J. Colloid Interface Sci.* **1974**, *46*, 111−117.

https://doi.org/10.1021/acsomega.1c01147
ACS Omega 2021, 6, 15770−15781

(40) Rodriguez-Garcia, M. E.; Londoño-Restrepo, S. M.; Ramirez-Gutierrez, C. F.; Millan-Malo, B. *Effect of the Crystal Size on the X-ray Diffraction Patterns of Isolated Orthorhombic Starches: A-Type. 2019*, arXiv:1808.02966v2. https://arxiv.org/abs/1808.02966 (assessed May 16, 2021).
(41) Vogt, F. G.; Brum, J.; Katrincic, L. M.; Flach, A.; Socha, J. M.; Goodman, R. M.; Haltiwanger, R. C. Physical, Crystallographic, and Spectroscopic Characterization of a Crystalline Pharmaceutical Hydrate: Understanding the Role of Water. *Cryst. Growth Des.* **2006**, *6*, 2333−2354.
(42) Cazzolli, G.; Caponi, S.; Defant, A.; Gambi, C. M. C.; Marchetti, S.; Mattarelli, M.; Montagna, M.; Rossi, B.; Rossi, F.; Viliani, G. Aggregation Processes in Micellar Solutions: A Raman Study. *J. Raman Spectrosc.* **2012**, *43*, 1877−1883.
(43) Mabrouk, K. B.; Kauffmann, T. H.; Aroui, H.; Fontana, M. D. Raman Study of Cation Effect on Sulfate Vibration Modes in Solid State and in Aqueous Solutions. *J. Raman Spectrosc.* **2013**, *44*, 1603−1608.
(44) Rebello, S.; Asok, A. K.; Mundayoor, S.; Jisha, M. S. Surfactants: Chemistry, Toxicity and Remediation. In *Pollutant Diseases, Remediation and Recycling*; Lichtfouse, E., Schwarzbauer, J., Robert, D., Eds., Springer: Switzerland, 2013; pp. 277−320.
(45) Katz, D. A. *The Science of Soaps and Detergents.* https://www.coursehero.com/file/14486561/Soap-and-detergent/ , 2000 (assessed January 6, 2021).
(46) Baviere, M.; Bazin, B.; Aude, R. Calcium Effect on the Solubility of Sodium Dodecyl Sulfate in Sodium Chloride Solutions. *J. Colloid Interface Sci.* **1983**, *92*, 580−583.
(47) Theodore, S.; Sai, P. S. T. Esterification of Ethanol with Sulfuric Acid: A Kinetic Study. *Can. J. Chem. Eng.* **2001**, *79*, 54−64.
(48) Liu, Y.; Lotero, E.; Goodwin, J. G., Jr. Effect of Water on Sulfuric Acid Catalyzed Esterification. *J. Mol. Catal. A: Chem.* **2006**, *245*, 132−140.
(49) Ghosh, S.; Roy, A.; Banik, D.; Kundu, N.; Kuchlyan, J.; Dhir, A.; Sarkar, N. How Does the Surface Charge of Ionic Surfactant and Cholesterol Forming Vesicles Control Rotational and Translational Motion of Rhodamine 6G Perchlorate (R6G ClO4)? *Langmuir* **2015**, *31*, 2310−2320.
(50) Afzal, M.; Kundu, P.; Das, S.; Ghosh, S.; Chattopadhyay, N. A Promising Strategy for Improved Solubilization of Ionic Drugs Simply by Electrostatic Pushing. *RSC Adv.* **2017**, *7*, 43551−43559.
(51) Lee, T.; Kuo, C. S.; Chen, Y. H. Solubility, Polymorphism, Crystallinity, and Crystal Habit of Acetaminophen and Ibuprofen by Initial Solvent Screening. *Pharm. Tech.* **2006**, *30*, 72−92.

https://doi.org/10.1021/acsomega.1c01147
ACS Omega 2021, 6, 15770−15781